JOURNAL OF GEOPHYSICAL RESEARCH, VOL. 103, NO. E9, PAGES 19,963–19,972, AUGUST 30, 1998

Ganymede's magnetosphere: Magnetometer overview

M. G. Kivelson,[1,2] J. Warnecke,[1] L. Bennett,[1] S. Joy,[1] K. K. Khurana,[1]
J. A. Linker,[3] C. T. Russell,[1,2] R. J. Walker,[1] and C. Polanskey[4]

Abstract. Ganymede presents a unique example of an internally magnetized moon whose intrinsic magnetic field excludes the plasma present at its orbit, thereby forming a magnetospheric cavity. We describe some of the properties of this mini-magnetosphere, embedded in a sub-Alfvénic flow and formed within a planetary magnetosphere. A vacuum superposition model (obtained by adding the internal field of Ganymede to the field imposed by Jupiter) organizes the data acquired by the Galileo magnetometer on four close passes in a useful, intuitive fashion. The last field line that links to Ganymede at both ends extends to ~2 Ganymede radii, and the transverse scale of the magnetosphere is ~5.5 Ganymede radii. Departures from this simple model arise from currents flowing in the Alfvén wings and elsewhere on the magnetopause. The four passes give different cuts through the magnetosphere from which we develop a geometric model for the magnetopause surface as a function of the System III location of Ganymede. On one of the passes, Ganymede was located near the center of Jupiter's plasma disk. For this pass we identify probable Kelvin-Helmholtz surface waves on the magnetopause. After entering the relatively low-latitude upstream magnetosphere, Galileo apparently penetrated the region of closed field lines (ones that link to Ganymede at both ends), where we identify predominantly transverse fluctuations at frequencies reasonable for field line resonances. We argue that magnetic field measurements, when combined with flow measurements, show that reconnection is extremely efficient. Downstream reconnection, consequently, may account for heated plasma observed in a distant crossing of Ganymede's wake. We note some of the ways in which Ganymede's unusual magnetosphere corresponds to familiar planetary magnetospheres (viz., the magnetospheric topology and an electron ring current). We also comment on some of the ways in which it differs from familiar planetary magnetospheres (viz., relative stability and predictability of upstream plasma and field conditions, absence of a magnetotail plasma sheet and of a plasmasphere, and probable instability of the ring current).

1. Introduction

The Galileo Orbiter has completed its reconnaissance of Jupiter's largest moon, Ganymede. The existence of an internally generated magnetic field large enough to surround Ganymede with a minimagnetosphere carved out of Jupiter's magnetosphere has been confirmed [*Kivelson et al.*, 1996, 1997; *Frank et al.*, 1997; *Gurnett et al.*, 1996; *Williams et al.*, 1997a, b]. Here we focus on the properties of this unique magnetosphere. Four passes at significantly different locations both relative to the Moon's surface and relative to the magnetosphere itself, supplemented by a distant crossing of Ganymede's wake in the flowing plasma of Jupiter's magnetosphere, enable us to present a model of its bounding surface, the magnetopause.

Near Ganymede's orbit (at a distance of 14.97 R_J from Jupiter, with Jupiter's radius ($R_J \equiv 71{,}492$ km), the Alfvén Mach number of Jupiter's magnetospheric plasma is < 1, implying that it is predominantly magnetic pressure rather than dynamic pressure that confines Ganymede's magnetosphere (see plasma parameters tabulated by F. Bagenal and F. Crary at URL: http://dosxx.colorado.edu/Galileo/encounter.html). As Ganymede's magnetosphere provides an example, thus far unique, in which the interaction between a magnetized body and a flowing plasma is dominated by the magnetic energy density, there is considerable incentive to describe its features quantitatively. Of particular importance are the plasma currents that flow in the interaction region, principally on the magnetopause. A first step in understanding those currents is to establish the shape of the magnetopause on which they flow. Knowledge of magnetopause currents will ultimately enable us to improve estimates of the internal field of Ganymede and possibly to identify some of the higher order multipole moments. At present, we fit Ganymede's internal magnetic field to lowest order as a centered dipole whose north pole is tilted 10° from the spin axis toward 200° Ganymede east longitude and whose equatorial surface field strength is 750 nT [*Kivelson et al.*, 1996]. By convention, the longitude is measured from 0° in the Jupiter-facing meridian plane through Ganymede and Jupiter. Ganymede's field, northward-oriented near the equator, is strong enough to stand off the Jovian magnetospheric field and the plasma in which it is embedded at an equatorial distance of roughly 2 R_G (R_G, radius of Ganymede ≡ 2631 km).

Because Jupiter's magnetic moment tilts 10° from its spin axis, the orientation and magnitude of the field and the plasma properties near Ganymede's orbit vary with the ~10.5 hour synodic period of Jupiter's rotation. Correspondingly, Ganymede's magnetosphere changes shape in a periodic and predictable manner, unlike the unpredictable variation that the solar wind imposes on a planetary magnetosphere. By adding Ganymede's dipole field to the magnetic field of Jupiter's magnetosphere at Ganymede's position (obtained from a field model), we obtain a simple and useful, though incomplete, representation. The model background field is taken from *Khurana* [1997]; it represents Jupiter's internal field with the O6

[1]Institute of Geophysics and Planetary Physics, University of California, Los Angeles.
[2]Department of Earth and Space Sciences, University of California, Los Angeles.
[3]Science Applications International Corporation, San Diego, California.
[4]The Jet Propulsion Laboratory, Pasadena, California.

Paper number 98JE00227.
0148-0227/98/98JE-00227$09.00

field model of *Connerney* [1993] and uses a Euler potential to represent the external magnetodisc field. Figure 1 shows modeled field lines and the Galileo trajectory projected into the 0° - 180° meridian plane in this vacuum superposition model for the four passes G1, G2, G7, and G8, the numbers referring to the orbits on which close passes of Ganymede (G) occurred. The direction of upstream plasma flow is out of the plane of the figure. Although the schematic magnetosphere, confined within a separatrix surface that corresponds to a magnetopause, differs in shape from representations of the magnetospheres of Earth and other planets, the topology corresponds closely. Outside the magnetopause are field lines that do not connect to the interior. For the terrestrial magnetosphere, such field lines would be solar wind field lines. Here they are field lines connected to Jupiter's ionosphere at both ends. Within the magnetosphere are closed field lines, i.e., ones connected to Ganymede at both ends, analogs of the low-latitude field lines in the terrestrial magnetosphere. Finally, there are field lines that connect to Ganymede at only one end and to Jupiter at the other end. They link to Ganymede's polar caps like the polar cap field lines in the terrestrial magnetosphere, and they form a region topologically equivalent to the lobes of the terrestrial magnetosphere. In an orthogonal view of the model in the meridian plane through Ganymede and Jupiter, the vacuum superposition model magnetosphere is roughly symmetric about the direction of the Moon's spin axis. Evidently, the presence of plasma produces departures from the simple models shown here, especially on scale sizes small compared with the diameter of the Moon.

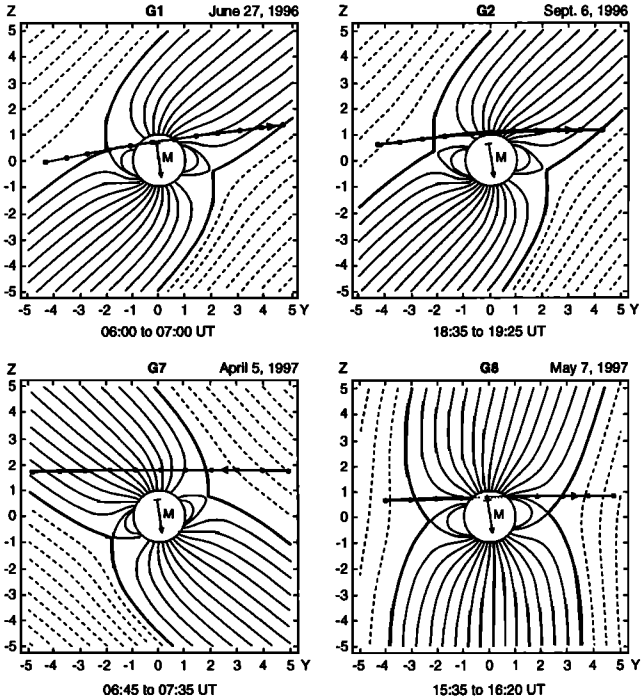

Figure 1. Field lines in a vacuum superposition of an external magnetic field from a model of Jupiter's magnetospheric magnetic field [*Khurana*, 1997] and the field of a Ganymede-centered magnetic dipole with equatorial surface field strength of 750 nT tilted 10° inward from -z, the direction antiparallel to Jupiter's spin axis. The view is a projection into the meridian plane of Jupiter through Ganymede's center. The four passes G1, G2, G7, and G8 are shown in panels as labeled. The orientation of the external field differs for the different passes. For the G1 (downstream) pass and G2 (polar) pass, the external field is ~120 nT and is tilted by ~50° outward from -z. For the G7 (polar) pass, the external field is again ~120 nT but is tilted inward by 50°. For the G8 (upstream) pass, the external field is ~75 nT and nearly due southward. For each case the projected trajectories of Galileo are shown with start and end times indicated and dots at 5-min intervals along the trajectory. Dashed field lines are those connected to Jupiter at both ends. Solid lines are connected to Ganymede at one or both ends. A surface separates these two classes of field lines, and its intersection with the plane of the figure is shown as a thick line. This surface provides a low-order approximation to the location of the magnetopause

2. Magnetometer Measurements From the Ganymede Passes

In order to optimize science return, Galileo's fields and particles instruments normally return data directly at relatively low rates whenever tracking is available. However, for roughly 1 hour at each satellite encounter, the data are stored on the spacecraft tape recorder at high time resolution. Thus for ~1 hour at each Ganymede pass, magnetometer vectors are acquired every 0.33 s. The three components of the magnetic field and the field magnitude measured on the G1 (June 27, 1996) [*Kivelson et al.*, 1996], G2 (September 6, 1996) [*Kivelson et al.*, 1997], G7 (April 5, 1997), and G8 (May 7, 1997) passes are plotted in Figure 2. The coordinate system is defined in the legend. In each plot, shading emphasizes the relatively abrupt field rotations that occur when the spacecraft crosses the Ganymede magnetopause.

Differences in the field signatures on the different passes are obvious in the plots of Figure 2. The orientation of the unperturbed background magnetic field varies with the System III longitude of the closest approach; the amplitude of the signature varies principally with the distance of closest approach. Times and locations of closest approach for each pass are given in Table 1. In the G2 pass with closest approach at 1.1 R_G (measured from the center of Ganymede) at 79.3° Ganymede latitude, the background external field was ~113 nT and the maximum field measured within the magnetosphere reached 1167 nT. In the G7 pass with closest approach at 2.18 R_G at 55.8° Ganymede latitude, the background external field was ~105 nT, and the maximum field measured within the magnetosphere was only ~220 nT. The vacuum-superposition model, also plotted for all of the passes in Figure 2, provides a fair estimate of the magnetic field other than near-boundary crossings, particularly for the high-latitude passes (G2 and G7). For these latter passes the difference between the measured and model x components is systematically negative. We can account for this feature of the data in terms of an Alfvén wing interaction [*Neubauer*, 1980; *Southwood et al.*, 1980]. Currents in the Alfvén wing bend back the flux tubes linked to the moon in the direction of the plasma flow both above and below, thereby introducing a negative (positive) B_x perturbation above (below) Ganymede. (The Alfvén wing currents can also contribute to B_y.) As the G2 and G7 passes occurred well above Ganymede's equator, the Alfvén wing contributed negative x perturbations.

The departures from the vacuum field model are less readily interpreted for G1 and G8. Both of these passes traversed regions close to the boundary between closed and open field lines (see Figure 1). The G8 pass occurred near the center of the plasma torus, and the ambient plasma was probably denser than on the other passes. Closest approach occurred at 1.61 R_G at 28.3° Ganymede latitude; the background external field was only ~90 nT, and the maximum field encountered within the magnetosphere was ~170 nT. The model field differs considerably from the measured field. The magnetopause encounters occurred ~10 min later inbound and earlier outbound than the times predicted from the vacuum superposition model. By contrast, for G1, G2, and G7, which all occurred well off the center of the plasma torus where the plasma density was

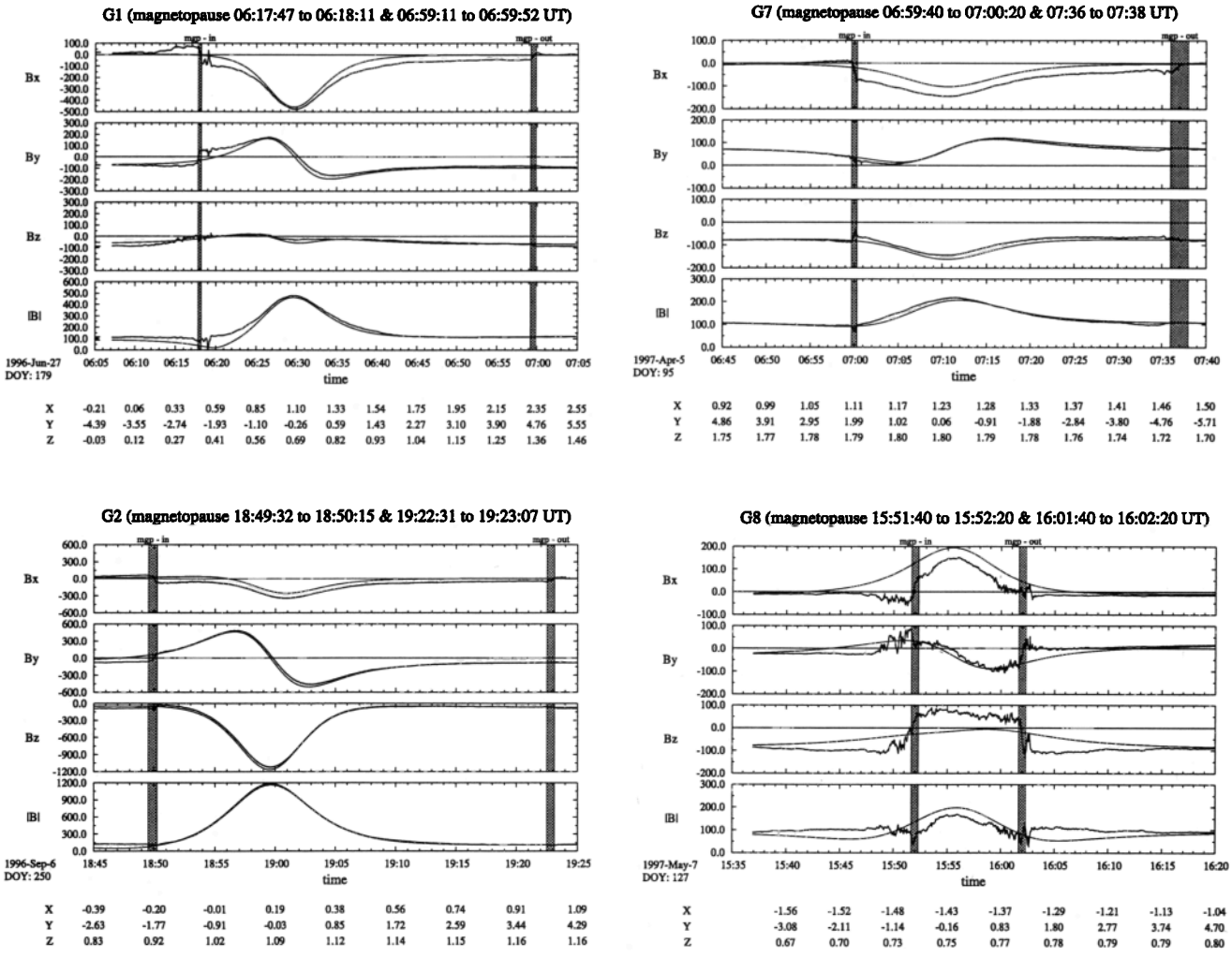

Figure 2. Components and magnitude of the magnetic field (in nT) measured by the Galileo magnetometer [*Kivelson et al.*, 1992] on Ganymede passes (a) G1 on June 27, 1996, (b) G2 on September 6, 1996, (c) G7 on April 5, 1997, and (d) G8 on May 7, 1997. The data are plotted as heavy lines in a Ganymede-centered coordinate system with z aligned with Jupiter's spin axis, x azimuthal and positive along the corotation direction, and y radially in toward Jupiter. Data are plotted versus. UT at the spacecraft. Rotations that we identify as magnetopause crossings are shaded. The components and magnitude along the orbit from the vacuum superposition model are plotted as thin lines. The figures are labeled with distances in R_G.

Table 1. Times and Locations Relative to Ganymede and to Jupiter of Closest Approach for the Four Galileo Passes

Pass	G1	G2	G7	G8
Date and time	June 27, 1996 - 0629:07	Sept. 6, 1996 - 1859:34	April 5,1997 - 0709:58	May 7, 1997 - 15:56:09
Altitude	838	264	3105	1599
Latitude	30.40	79.30	55.79	28.31
East longitude	247.5	237.3	271.3	85.8
Local time	1116	1046	1944	0807
Jupiter east longitude	185	202	340	73

Passes are labeled G1, G2, G7, and G8, the numbers identifying the orbit on which the encounter occurred. Altitude is given in kilometers, latitude and longitude relative to Ganymede's surface in degrees, local time in hours. Longitudes <180° are upstream of Ganymede relative to the direction of magnetospheric plasma flow. Ganymede's location relative to Jupiter is given by its east longitude in degrees (relative to the origin of System III) and the local time of the encounter in hours and minutes.

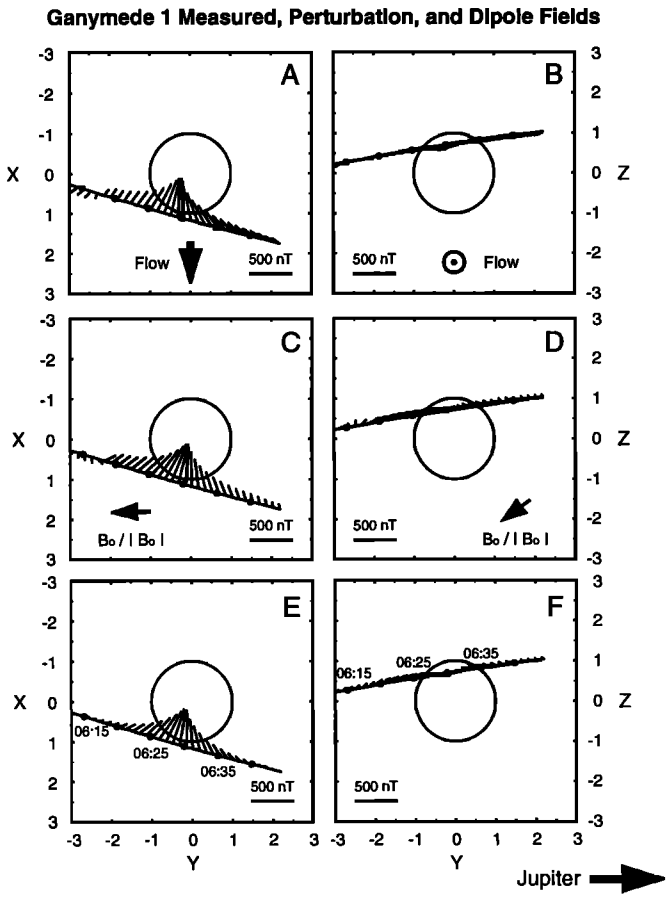
Ganymede 1 Measured, Perturbation, and Dipole Fields
A
B
C
D
E
F
Flow
500 nT
Bo / | Bo |
06:15
06:25
06:35
X
Y
Z
Jupiter

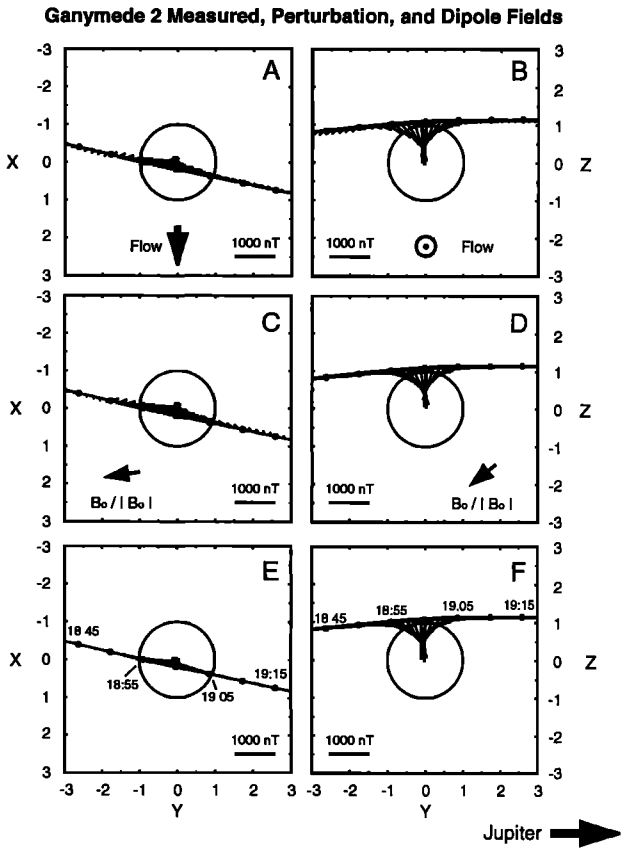
Ganymede 2 Measured, Perturbation, and Dipole Fields
A
B
C
D
E
F
Flow
1000 nT
Bo / | Bo |
18 45
18:55
19 05
19:15
X
Y
Z
Jupiter

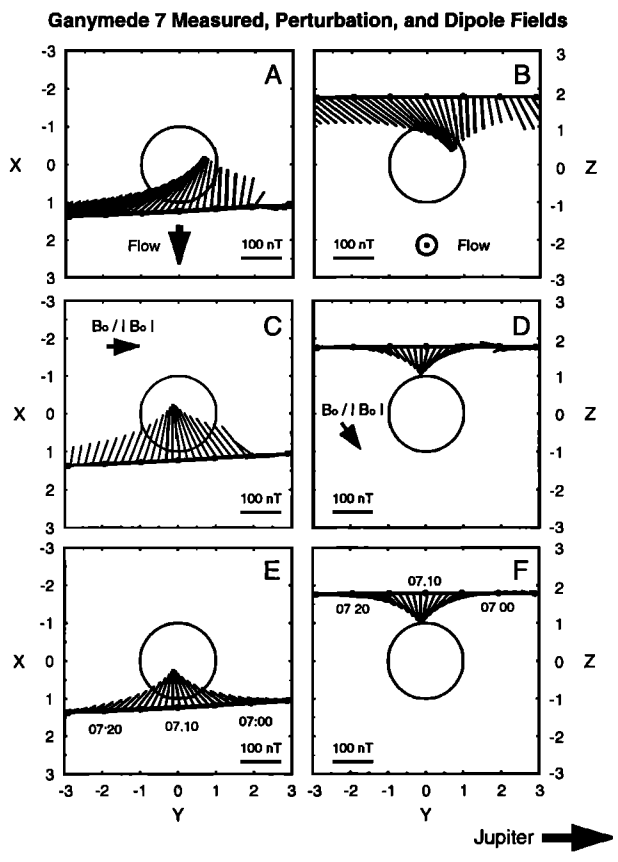
Ganymede 7 Measured, Perturbation, and Dipole Fields
A
B
C
D
E
F
Flow
100 nT
Bo / | Bo |
07:20
07.10
07:00
X
Y
Z
Jupiter

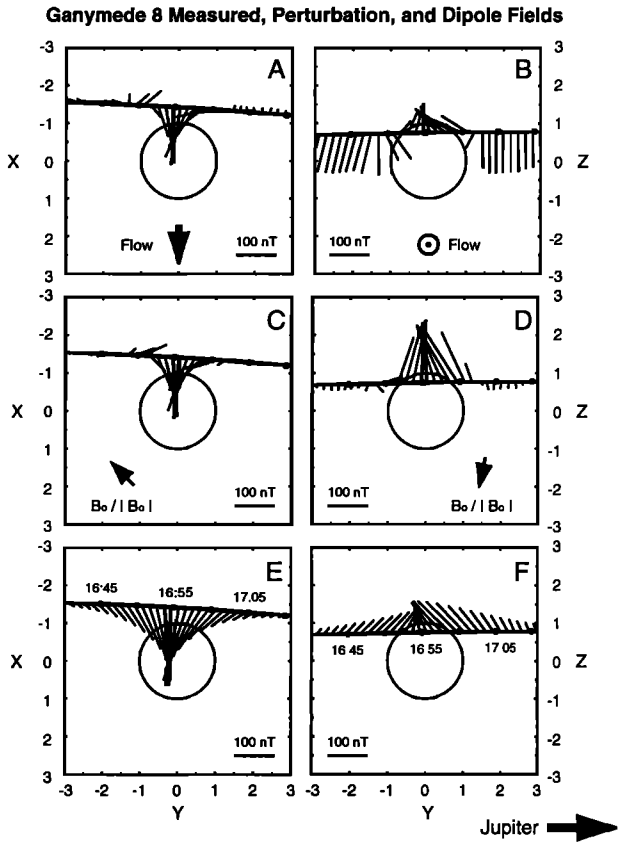
Ganymede 8 Measured, Perturbation, and Dipole Fields
A
B
C
D
E
F
Flow
100 nT
Bo / | Bo |
16:45
16:55
17.05
X
Y
Z
Jupiter

relatively low, the magnetopause crossings occurred within ~2 min of the times inferred from the vacuum-superposition model. Fluctuations were small within the magnetosphere for all passes other than G8.

The geometry of all four passes is illustrated in Figure 3. The trajectories have been projected into Ganymede's equatorial plane (x-y) and the Ganymede-Jupiter meridian plane (y-z). The G1 wake pass occurred downstream in the flow. G2 and G7 were polar passes with G2 at very low altitude (closest approach at 0.1 R_G altitude) and G7 at higher altitude. G8 was an upstream pass relative to the direction of the corotating magnetospheric plasma. Thus the collective coverage of the magnetosphere was quite extensive. In the top pairs of panels, projections of measured magnetic field vectors (1min averages) are shown as arrows rooted at successive locations along the trajectory. In the middle pair of panels the background field has been subtracted, and just the Ganymede-associated perturbations remain. In the bottom pair of panels the model field perturbations along the trajectory are plotted. The perturbations (middle panels) and the model (bottom panel) are in agreement except for the bend-back in the x component. This effect, attributed to Alfvén-wing currents, is apparent for G2 and is extreme for the most distant pass, G7, where the internal field contribution is comparatively small and the Alfvén wing current system is well developed. Additional discrepancies (local rotations) are evident at magnetopause crossings.

As we noted above, the vacuum-superposition model is less satisfactory for the G8 pass (Figure 3d) than for the other passes. We have attributed this, in part, to the locations of the different encounters relative to Jupiter's plasma sheet. Encounters G1, G2, and G7 occurred in a low-plasma β environment (β is the ratio of plasma thermal pressure to magnetic pressure) where the vacuum-superposition model provides useful guidance. The G8 encounter occurred in a higher plasma β environment near the center of the plasma sheet where the vacuum-superposition model departs considerably from observations. The dynamic pressure of the plasma, neglected in the vacuum-superposition model, compresses the magnetosphere, moving the magnetopause inward of the location of the separatrix that is the effective magnetopause in the vacuum superposition model. This compression accounts for the large shift between the predicted and actual times of magnetopause crossings on this pass. In addition, the G8 trajectory lay just within the magnetopause at relatively low latitude. In the upstream, low-latitude magnetosphere, magnetopause currents enhance the z component of the field inside the boundary and decrease the x component. Figure 4 shows schematically how the dayside magnetopause currents at Earth modify a dipole field. This type of distortion produces the differences in orientation between the measured and model field vectors plotted in panels D and F of Figure 3d. The large fluctuations of the field recorded through the entire G8 close pass (see Figure 2b) are consistent with the pass having occurred just inside of the upstream magnetopause boundary where effects of boundary motions and currents were important. The schematic also suggests that the spacecraft encountered closed field lines in the actual field configuration represented on the right even though it would not have penetrated closed field lines in the vacuum superposition model represented on the left. Such a closed field configuration is consistent with the identification near closest approach of butterfly distributions of trapped electrons [*Williams et al.*, 1997b].

The low-latitude upstream magnetopause encountered on G8 inbound provides the closest parallel to the low-latitude dayside magnetopause investigated extensively for the terrestrial magnetosphere [*Berchem and Russell*, 1982; *Phan and Paschmann*, 1996]. There it has been found that the typical thickness is ~900-1400 km, or 10 to 30 times the Larmor radius of a magnetosheath proton (ρ_{Lp}) At Ganymede the inbound G8 crossing lasted < 40 s, which implies that the boundary was < 400 km thick if the surface was at rest in Ganymede's frame. (The presence of multiple crossings and partial crossings of the outbound magnetopause reveals that the boundary moves. Thus our estimate, which overlooks the effect of normal motion of the boundary, is an approximation. However, because the duration of the observed crossings varied little, the effect is probably unimportant.) The Larmor radius for ions of mass ≈ 16 proton masses (ρ_{Li}) in a plasma flowing at ~150-180 km/s [*Williams et al.*, 1997a; *Frank et al.*, 1997] with a background field ~100 nT is ~160-190 km. Thus at Ganymede the magnetopause thickness is only $\approx 2\rho_{Lp}$ Electrons are less energetic, and their gyroradii (ρ_{Le}) are small compared with the boundary thickness.

3. Magnetopause Geometry

Most of the magnetopause crossings are distinctly evident as sharp field rotations whose locations are given in Table 2. The coordinate system is one that organizes them in relation to the external field orientation. Here X is along the flow, Z is selected so that the external field lies in the X-Z plane, and Y is orthogonal to the other two directions. The eight magnetopause crossings are used to fit a model of the magnetopause surface.

In selecting a form for the magnetopause model, we have been guided by a magnetohydrodynamic simulation for the external field orientation representing the G1 flyby based on the simulation code described by *Linker et al.* [this issue]. Figure 5 shows cuts through the surface that contain all field lines connected to Ganymede in the simulation. Cuts through the boundary in XY planes at different values of Z give ovoid cross sections. Cuts through constant Y show a north-south tilt away from Ganymede in the direction of corotation (i.e., the tilt imposed by the Alfvén-wing current system [*Neubauer*, 1980; *Southwood et al.*, 1980]). They also reveal a north-south asymmetry of the boundaries in Jupiter's meridian plane with the boundary displaced farther away from Jupiter above Ganymede than below. This north-south asymmetry also appears in the meridional cut through the vacuum superposition model shown in Figure 1 (G1); passes G2, G7, and G8 indicate that the asymmetry varies with the external field orientation. The

Figure 3. Measured magnetic field and measured and modeled magnetic field perturbations at Galileo during the closest approach to Ganymede during encounters (a) G1, (b) G2, (c) G7, and (d) G8. The lines with solid circles show Galileo's position at 5-min intervals along its trajectories past Ganymede. The trajectories are plotted in the coordinate system described in Figure 2. The trajectory is projected into the x-y plane for diagrams A, C, and E and into the y-z plane for diagrams B, D, and F. Diagrams A and B show projections of 1 min averages of the measured magnetic field drawn from the measurement locations. Note that the scale of these projections is given in each panel, and different scales are used for the different passes. A fit to the trend of the background field data was subtracted from the observed field to provide perturbation field vectors that are similarly plotted as 30 s averages in diagrams C and D. Projections of the model Ganymede-centered dipole magnetic field vectors are similarly plotted as 30 s averages in diagrams E and F. The background field of Jupiter's magnetosphere was southward oriented at different tilts for the four passes. The direction of the projected background field is indicated by arrows in diagrams C and D.

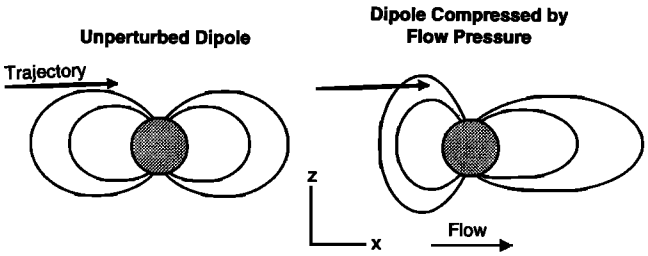

Figure 4. Schematic illustration of the way in which the pressure of flowing plasma (shown flowing from the left) affects the form of an initially dipolar magnetic field configuration. The trajectory of Galileo during the G8 encounter is shown schematically. Near the trajectory the effect of dynamic pressure is to decrease B_x and increase B_z, as occurred in the G8 pass. As the pass skimmed the boundary between closed and open field lines in the model shown in Figure 1, these distortions should cause Galileo's trajectory to penetrate into the region of field lines closed at both ends at Ganymede. In the region downstream of the dipole source, the field lines stretch along the flow direction.

asymmetry present in Figure 5 applies when Ganymede is above Jupiter's current sheet. When Ganymede is below Jupiter's current sheet, as for G7, the magnetopause northward of Ganymede is shifted toward Jupiter.

Our fits to the observations use a functional form that depends on the external field orientation and allows for the ovoid cross section in planes normal to Z, the Alfvén wing tilt, and the north-south asymmetry. We define the surface as

$$f(X,Y,Z) = \frac{(X - X_0)^2}{a^2} + \frac{(Y - Y_0)^2}{b^2} = 1 \qquad (1)$$

where the offset (X_0, Y_0) of the center of the ellipse depends on Z. We take

$$X_0(Z) = X_0(0) + |Z| \tan\theta \qquad (2)$$

where θ characterizes the bend-back of the magnetopause. In the Alfvén-wing description, this angle should satisfy tan $\theta = M_A$, but we take it as a parameter to be determined. We adopt a form of the Y offset that depends on the System III east longitude (ϕ) of the encounter in order to allow the north-south asymmetry to vary with the external field orientation:

$$Y_o(Z) = \frac{2}{\pi} Y_{o,\max} \sin(\phi - 248^\circ) \arctan(Z/\lambda) \qquad (3)$$

This offset is nearly constant for $|Z| >> \lambda$ and is greatest at ϕ = 158° (Ganymede above the current sheet) and 338° (Ganymede below the current sheet).

In principle, a least squares inversion algorithm can fit all six parameters (a, b, $X_o(0)$, $Y_{o,\max}$, λ, and θ) given the locations of the eight magnetopause crossings. However, the lack of downstream crossings near $Y = 0$, $Z = 0$ introduces uncertainty into the fits, yielding values that inflate the magnetosphere considerably relative to the simulation results. By setting $a = 2.2\ R_G$ and $\lambda = 0.5\ R_G$, and calculating the remaining parameters by the least squares method, we obtain a surface form similar to that of the simulation. The calculated parameters are $X_o(0) = 0.544$, $Y_{o,\max} = 0.914$, (all in R_G) and $\theta = 0.298$ radians. Table 3 gives the value of f (equation (1)) at each crossing. For f close to 1, the fit is good. The only two crossings for which f differs from 1 by more than 12% are inbound G1 and inbound G2, both of which occurred near the polar cusp (see Figure 1), where the surface location is a sensitive function of position, and large errors are expected.

A satisfactory representation of the magnetopause should predict the normal directions reasonably accurately. Table 3 gives the angles between the model normals and the measured normals for each crossing. The measured normals are entered in Table 2. They were obtained by rotating the data for each magnetopause crossing into a minimum variance coordinate system. The quality of the estimate is also indicated. If the normal direction is ill defined (i.e., the ratio of the intermediate to minimum eigenvalues of the rotation matrix is less than an order of magnitude), or if it is difficult to identify the boundary rotation in the data, the quality of the normal is shown as poor. The angle between the model and measured normals is large for G1 inbound and G7 outbound. For G1 inbound the proximity to the polar cusp boundary again can be appealed to as the source of the discrepancy because the curvature of the magnetopause changes rapidly with distance along the surface in this region. For G7 outbound the rotation is poorly defined, and the discrepancy between the model and the minimum variance normal may result from a poorly constrained observation. The form of the model magnetopause differs considerably from the form of Earth's

Table 2. Magnetopause Crossing Positions for the Four Ganymede Passes

	East Longitude	X, RG	Y, RG	Z, RG	nx	ny	nz	Quality	Date t, UT
G1 in	191.27	0.486	-1.774	-1.434	0.30	-0.30	-0.91	good	June 27, 1996 0618
G1 out	167.34	2.354	2.176	4.444	-0.27	0.96	-0.05	poor	June 27, 1996 0700
G2 in	207.39	-0.201	-1.922	-0.556	-0.73	-0.49	-0.47	good	Sept. 6, 1996 1850
G2 out	188.59	1.021	2.057	-3.571	-0.14	0.75	0.64	poor	Sept. 6, 1996 1923
G7 in	345.66	1.115	2.656	-0.325	-0.11	0.75	-0.65	fair	April 5, 1997 0700
G7 out	324.59	1.469	-2.082	5.000	0.30	0.08	0.95	poor	April 5, 1997 0737
G8 in	75.87	-1.461	-0.834	0.636	-0.72	-0.55	0.43	good	May 7, 1997 1552
G8 out	70.17	-1.336	1.109	0.925	-0.70	0 51	0.50	good	May 7, 1997 1602

The east longitude of Ganymede relative to the origin of System III is given. (Equator crossings occur at 68° and 248°). Here X is along corotation flow, the Z direction is chosen so that the local background field lies in the XZ plane, and Y is orthogonal to X and Z and positive inward toward Jupiter. The components of the normal vectors have been determined from minimum variance analysis. The quality of the normal determination is indicated, and the UT of the crossing is given.

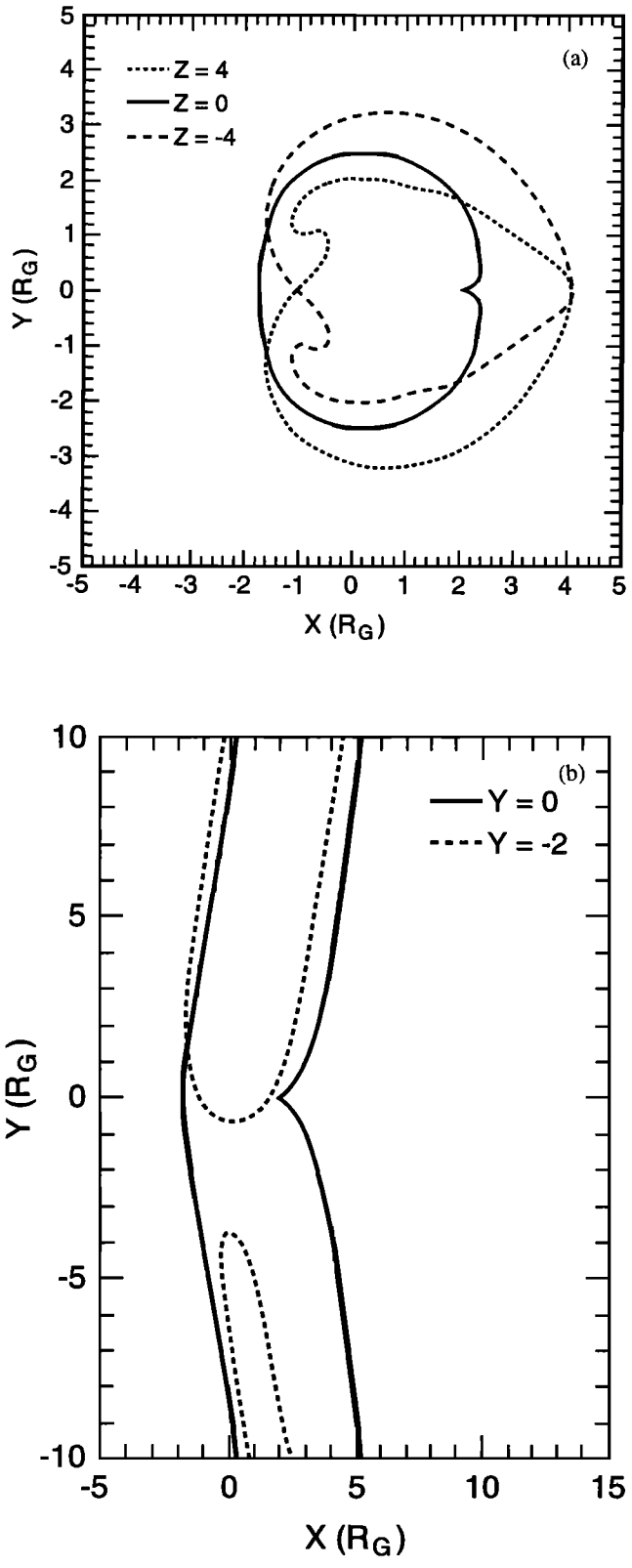

Figure 5. Cuts through the boundary that encloses all field lines linked to Ganymede in an MHD simulation based on the simulation code described by *Linker et al.* [this issue]. The external field orientation corresponds to the case of the G1 encounter. (a) Cuts perpendicular to the Z axis for different Z values (in R_G) labeled on the figure. (b) Cuts perpendicular to the Y axis at two different values of Y. The north-south asymmetry of the boundary is clear.

magnetopause as anticipated from the representations of Figure 1. Whereas Earth's magnetopause is roughly symmetric about the flow direction because the solar wind dynamic pressure confines it, both the dynamic pressure and the magnetic pressure of the external field control Ganymede's magnetopause. This imposes a small but distinct anisotropy about the flow direction. The bend-back angle of 0.298 radians = 17.1° away from the equatorial plane is constrained predominantly by data from encounters G1, G2, and G7, all of which occurred at relatively high Ganymede magnetic latitudes. The value is consistent with an Alfvén Mach number of 0.31, a reasonable value for the encounters away from the center of the plasma sheet (the range 0.23-0.93 is given by F. Bagenal and F. Crary, http://dosxx.colorado.edu/Galileo/encounter.html).

It must be emphasized that the closure of the magnetopause in the wake was forced to correspond to simulation and may be greatly oversimplified in the model presented here. Indeed, a substantial magnetic signature recorded as Galileo passed through Ganymede's wake at a downstream distance of 30 R_G on June 26, 1997, suggests that plasma at pressures above ambient, possibly heated by reconnection in the downstream Ganymede magnetosphere, was present in the distant wake (*K. K. Khurana et al.*, Ganymede's distant wake, submitted to Journal of Geophysical Research, 1997).

4. Ultralow Frequency Waves on the Magnetopause

On all four Ganymede passes the power in field fluctuations increased near magnetopause crossings, but on most passes even near the boundary the amplitude of the waves remained small (see, for example, the G7 pass shown in Figure 2c). However, on the G8 pass that occurred near the center of the Jovian plasma sheet, waves of 10-20 nT with periods of 15-20 s were present near both the inbound and outbound magnetopause crossings (Figure 2d). An appropriate coordinate system for examining waves on the boundary is a principal axis system with L along the direction of maximum variance across the boundary, N along the direction of minimum variance, and M orthogonal to the other two. The data for the inbound G8 magnetopause in this boundary normal coordinate system are plotted in Figure 6. This is a clean crossing with a well-defined normal direction. Waves are evident just outside the boundary. They are predominantly transverse, with smaller amplitude in the field magnitude than the components. The waveforms are irregular, but the M and N components vary in-phase with each other, while the L component varies in quadrature (90° out of phase) with the other components. Such phase relations are expected for a surface wave propagating along the M direction on a tangential discontinuity. Displacement of the magnetopause boundary could result from pressure/density fluctuations in the torus plasma, but the perturbations are periodic, as would be expected if they arise from the instability of a surface in a shear flow. The wavelength can be estimated by neglecting the spacecraft velocity and recalling that the phase velocity of a Kelvin-Helmholtz wave is half the relative flow velocity on the two sides of the boundary. With the plasma sheet plasma flowing at 150 km/s relative to Ganymede [*Williams et al.*, 1997a], the wavelength is 1125 km, or roughly 0.5 R_G, which is a plausible scale size for a surface wave perturbation on magnetopause at 2 R_G from the central body.

The amplitude of surface waves is larger on the G8 pass than on other passes, consistent with the previously discussed location near the center of Jupiter's plasma sheet. G8 was the only pass for which the flow kinetic energy incident on Ganymede's magnetosphere was large, and it is flow energy of the external plasma that drives the surface waves. The appearance of Kelvin-Helmholtz surface waves at Ganymede is of particular theoretical interest because it extends the study of such waves into a regime

Table 3. Magnetopause Normals Evaluated for the Model Magnetopause of Equation (1) With a = 2.20, b = 2.90, $X_o(0) = 0.544$, $Y_o(0) = 0.914$, $\lambda = 0.500$ *(All in* R_G*), and* $\theta = 0.298$ *Radians at the Crossing Positions of the Four Ganymede Passes*

	East Longitude	X, R_G	Y, R_G	Z, R_G	$n_{model,x}$	$n_{model,y}$	$n_{model,z}$	f	$n \cdot n_{model}$
G1 in	191.27	0.486	-1.774	-1.434	-0.337	-0.920	-0.201	0.718	0.357
G1 out	167.34	2.354	2.176	4.444	0.249	0.966	-0.063	1.115	0.857
G2 in	207.39	-0.201	-1.922	-0.556	-0.529	-0.741	-0.414	0.766	0.944
G2 out	188.59	1.021	2.057	-3.571	-0.361	0.924	0.129	0.990	0.826
G7 in	345.66	1.115	2.656	-0.325	0.218	0.790	-0.573	1.102	0.941
G7out	324.59	1.469	-2.082	5.000	-0.342	-0.933	0.116	1.082	-0.067
G8 in	75.87	-1.461	-0.834	0.636	-0.942	-0.187	0.278	1.069	0.901
G8 out	70.17	-1.336	1.109	0.925	-0.918	0.275	0.285	1.119	0.926

Position information is as in Table 2; f is the value of the fit function at the crossing location. The column $\mathbf{n} \cdot \mathbf{n}_{model}$ gives the cosine of the angle between model and measured normals. Values near 1 for f and $\mathbf{n} \cdot \mathbf{n}_{model}$ imply good fits.

in which the thickness of the oscillating boundary is of the order of the ion gyroradii in one of the bounding plasmas.

5. Ultralow Frequency Waves in the Upstream Magnetosphere

Both the field orientation and the angular distribution of energetic electrons [*Williams et al.*, 1997b] suggest that Galileo encountered dipole-like Ganymede field lines (with both ends linked to Ganymede) on the G8 pass. Analogy to Earth's magnetosphere suggests that transverse field perturbations in the band of frequencies imposed by field line resonances may be detectable. However, the rapid motion of Galileo across Ganymede L-shells would broaden narrow-banded frequency peaks, so truly wave-like fluctuations are unlikely. A rough

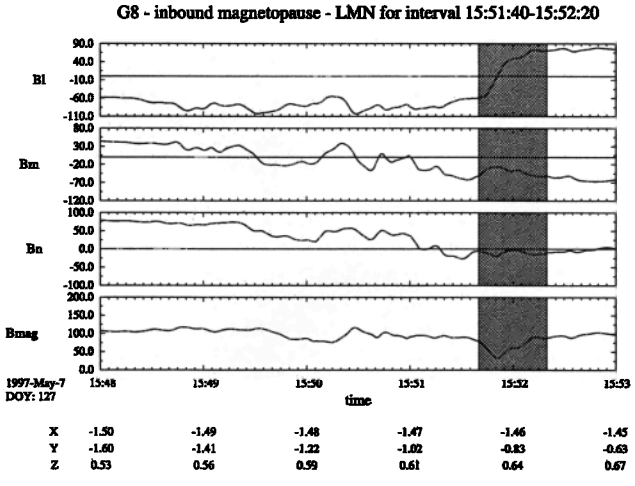

Figure 6. High-resolution plot of magnetic field data near the inbound magnetopause crossing on G8 revealing the boundary waves arising from possible surface wave oscillations on the magnetopause of Ganymede's magnetosphere on May 7, 1997, in magnetopause normal coordinates. (The magnetopause crossing occurred at ~1552 UT). Here *N* is the direction normal to the boundary determined from a minimum variance analysis, *L* is the direction of maximum variance across the boundary and the interval used to identify these directions is shaded. *M* is orthogonal to *L* and *N*.

estimate of the fundamental period (*T*) of standing shear Alfvén waves can be made as follows:

$$T \approx \oint ds / v_A \leq 2\ell(\mu_0 m_i n)^{1/2} / B \qquad (4)$$

where *s* is distance along the field line, v_A is the Alfvén speed, ℓ is the length of the field line, m_i is the ion mass, and *n* is the ion number density. As Ganymede is icy and ion sources within the magnetosphere are proton-rich compared with the plasma torus, we take $m_i \sim 10\ m_p$ (m_p is the proton mass). With $\ell = 1.5\ R_G$ and B = 150 nT, the fundamental period is of the order of $8(n(cm^{-3}))^{1/2} s$. Spectral analysis of the fluctuations within the magnetosphere reveals transverse power at periods longer than 4 s (frequencies below ~0.25) at levels significantly above the compressional power. This signature is consistent with generation by low harmonics of standing field line resonances. However, the cyclotron frequency of ions with $m_i/m_p \approx 8$-16 falls in the same frequency band as the proposed field line resonances. More extensive wave analysis is needed to interpret the source of the observed power in field fluctuations.

6. Reconnection

In an earlier report on the G1 and G2 passes [*Kivelson et al.*, 1997], we discussed the relation between the flow velocity over the polar cap and the reconnection rate at the nose of the magnetopause. Reconnection imposes some fraction of the upstream potential drop across Ganymede's magnetosphere, and the convection flow speed is directly proportional to the imposed potential drop. Velocity measurements [*Frank et al.*, 1997; *Williams et al.*, 1997a] thus constrain the reconnection efficiency, by which we mean the ratio ε of the imposed potential drop to the full possible potential drop across the width of the magnetosphere. For G2, *Frank et al.* [1997] report that the ambient plasma flows at 180 km/s and that the bulk flow velocity over the polar cap is 70 km/s. *Williams et al.* [1997a] report that the ambient plasma flows at 150 km/s and place an upper limit to the flow speed over the polar cap of ~25-45 km/s. We next explore the implications of these measurements for the reconnection efficiency of Ganymede's magnetosphere. We have previously noted [*Kivelson et al.*, 1997] that at high altitudes within the lobes of Ganymede's magnetosphere, the convective flow speed v_L is

$$v_L = E_L / B_0 = \varepsilon E_{cr} / B_0 \quad (5)$$

Here E_L is the convection electric field in the high-latitude lobe where the magnetic field strength does not differ from the external field magnitude B_o, and E_{cr} is the convection electric field in the unperturbed plasma that is flowing onto Ganymede's magnetosphere. The measured quantity [*Frank et al.*, 1997; *Williams et al.*, 1997a] provides v_{pc}, the flow speed at the low altitude of the second Ganymede pass. *Kivelson et al.* [1997] invoke an approximate form of flux-tube compression in a dipole field to show that along the G2 trajectory of Galileo, the flow is approximately

$$v_{pc} = \left(E_L/B_{pc}\right)(B_{pc}/B_o)^{1/2} = \varepsilon v_{cr}(B_o/B_{pc})^{1/2} \quad (6)$$

hence

$$\varepsilon = \left(v_{pc}/v_{cr}\right) \times \left(B_{pc}/B_0\right)^{1/2} \quad (7)$$

Near the center of the polar cap $B_{pc} \approx 10B_o$. The measured flows (selecting the upper limit when using the measurements of *Williams et al.* [1997a]) imply that $\varepsilon \approx 1$, an unexpectedly large value that should be taken as an upper limit. The high reconnection efficiency requires most of the plasma flowing onto Ganymede's magnetosphere to cross the magnetopause. Some plasma must be diverted around the magnetosphere because there is clear evidence of flow divergence on the flanks of the magnetosphere [*Frank et al.*, 1997], but our analysis suggests that a large fraction of the incident flow penetrates the boundary.

In a steady state the flux tubes that reconnected at the upstream neutral line must disconnect after they have convected to the downstream boundary. For this reason, we expect that a downstream neutral line, analogous to Earth's distant neutral line in the magnetotail, must be continuously active. Heated plasma must be ejected from this downstream neutral line, and we believe that it is this heated plasma that forms the wake detected on the distant wake crossing of June 26, 1997, as discussed by *Khurana et al.* [1997].

7. Ganymede's Internal Magnetic Field and the Polar Cap Boundary

The combined data set from four passes provides good support for our earlier estimates of the internal magnetic moment of Ganymede [*Kivelson et al.*, 1996]. The vacuum superposition model that we have used to organize and interpret our data does not and should not match the measurements in every detail. We have explained some of the departures from the simple model in terms of predictable effects of interaction with the ambient plasma. Furthermore, the internal field model [*Kivelson et al.*, 1997] predicts loss cones that are in generally good agreement with the loss cones observed in the energetic electron fluxes after correction for instrument response [*Williams et al.*, 1997a]. The lower energy electron loss cones do not follow predictions of the vacuum superposition model [*Frank et al.*, 1997] in measurements made immediately after the inbound magnetopause crossing and before the outbound crossing. However, the plasma in these regions, like boundary layer plasmas in Earth's magnetosphere, is controlled by source and loss mechanisms different from those that act deeper in the magnetosphere. Thus their properties do not provide a useful test of the magnetospheric field configuration.

The confirmation of the internal field model from the collective data sets allows us to describe the polar cap boundary and to indicate where the Ganymede aurora [*Hall et al.*, 1997] must be generated. The auroral symmetry axis should lie along the internal dipole whose north pole is tilted by 10° from the spin axis toward 200° Ganymede east longitude. (Longitude of 180° is radially outward from Jupiter.) The field lines that connect to Jupiter lie within ~30° of the north and south poles. Modification of the shape of the polar cap by tilts in the external field as Jupiter rotates about its axis are expected, but the dominant feature of the aurora is expected to be its approximate symmetry about the dipole axis.

8. Discussion

Ganymede provides an example of a magnetospheric interaction that cannot be found at Earth or other planets, one in which the upstream conditions are steady over times long compared with the time to convect plasma through the system and these stable conditions are predictable. The predictable upstream conditions allowed us to define a boundary shape despite the limited data set available for analysis. In future data analysis, there may be lessons relevant to the study of magnetic activity at Earth. It remains a challenge to determine if Ganymede's activity is intermittent or if the steady upstream conditions circumvent the development of bursty activity. Analysis of data from all Ganymede wake crossings may help resolve this question.

Ganymede's magnetosphere is different from Earth's for reasons other than the predictable nature of its environment. Its spatial structure differs greatly because of the low Alfvén Mach number of the torus plasma. Despite its unfamiliar spatial form, there are features such as the magnetic topology (closed and open field line regions) that have direct parallels in Earth's magnetosphere. Major differences are apparent and must not be overlooked. For example, the shape of the magnetosphere excludes the development of any equivalent of Earth's plasmasheet. As well, the slow rotation of Ganymede precludes the development of a plasmasphere as can be inferred from simple estimates. The velocity of corotation within Ganymede's magnetosphere (radius $\approx 2\ R_G$) is $\sim 4\pi R_G/T_G = 0.053$ km/s with T_G = 172 hours. The convective flow speed at low altitude above the polar cap is of the order of 70 km/s [*Frank et al.*, 1997], so much larger than the velocity of rotation about Ganymede that plasma will be convected from upstream to downstream everywhere, and no plasmasphere will form. On the other hand, energetic particles of tens of keV will drift in the magnetic field gradient at speeds that can exceed the convection speed. Such particles can, in principle, form a ring current, and in fact, energetic electrons with the double loss cone distributions of trapped ring current particles have been reported [*Williams et al.*, 1997b]. However, the gyroradii of the ions of high enough energy to develop closed drift orbits would be 4550 $(m_i/m_p)^{1/2}$ $E(\mathrm{keV})^{1/2}/B(\mathrm{nT})$ km ~500 km, a scale large compared with the characteristic lengths for field variations. Thus it seems likely that the ring current would be unstable to decay through violation of the adiabatic invariants. Further analysis of Ganymede's magnetosphere may show how the absence of stable plasma boundaries affects its dynamics.

Acknowledgments. The work reported here was partially supported by the Jet Propulsion Laboratory under contract JPL 958694. We acknowledge discussions with Vytenis Vasyliunas, whose insights contributed considerably to our interpretations. We thank one of the referees for suggesting revisions of our original presentation. UCLA Institute of Geophysics and Planetary Physics Publication 4931.

References

Berchem, J., and C. T. Russell, The thickness of the magnetopause current layer: ISEE 1 and 2 observations, *J. Geophys. Res.*, *87*, 2108, 1982.

Connerney, J. E. P., Magnetic fields of the outer planets, *J. Geophys. Res.*, *98*, 18,659, 1993.

Frank, L. A., W. A. Paterson, and K. L. Ackerson, Outflow of hydrogen ions from Ganymede, *Geophys. Res. Lett.*, *24*, 2151, 1997.

Gurnett, D. A., W. S. Kurth, A. Roux, S. J. Bolton, and C. F. Kennel, Evidence for a magnetosphere at Ganymede from plasma-wave observations by the Galileo spacecraft, *Nature*, *384*, 535, 1996.

Hall, D. et al., Ganymede aurora, *Astrophys. J. Lett.*, in press, 1997.

Khurana, K. K., Euler potential models of Jupiter's magnetospheric field, *J. Geophys. Res.*, *102*, 11,295, 1997.

Kivelson, M. G., K. K. Khurana, J. D. Means, C. T. Russell, and R. C. Snare, The Galileo Magnetic Field Investigation, *Space Sci. Rev.*, *60*, 357, 1992.

Kivelson, M. G., K. K. Khurana, C. T. Russell, R. J Walker, J. Warnecke, F. V. Coroniti, C. Polanskey, D. J. Southwood, and G. Schubert, Discovery of Ganymede's magnetic field by the Galileo spacecraft, *Nature*, *384*, 537, 1996.

Kivelson, M. G., K. K. Khurana, F. V. Coroniti, S. Joy, C. T. Russell, R J. Walker, J. Warnecke, L. Bennett, and C. Polanskey, The magnetic field and magnetosphere of Ganymede, *Geophys Res. Lett.*, *24*, 2155, 1997.

Linker, J. A., K. K. Khurana, M. G. Kivelson, and R. J. Walker, MHD simulations of Io's interaction with the plasma torus, *J. Geophys. Res.*, this issue.

Neubauer, F. M., Non-linear standing Alfven wave current system at Io: Theory, *J. Geophys. Res. 85*, 1171-1178, 1980.

Phan, T. D., and G. Paschmann, Low-latitude dayside magnetopause and boundary layer for high magnetic shear, 1, Structure and motion, *J. Geophys. Res.*, *101*, 7801, 1996.

Southwood, D. J., M. G. Kivelson, R. J. Walker, and J. A. Slavin, Io and its plasma environment, *J. Geophys. Res.*, *85*, 5959-5968, 1980.

Williams, D. J., et al., Energetic particle signatures at Ganymede: Implications for Ganymede's magnetic field, *Geophys. Res. Lett.*, *24*, 2163, 1997a.

Williams, D. J., B. H. Mauk, and R. W. McEntire, Trapped electrons in Ganymede's magnetic field, *Geophys. Res. Lett.*, *24*, 2953, 1997b.

L. Bennett, S. Joy, K. K. Khurnana, M. G. Kivelson, C. T. Russell, R. J. Walker, and J. Warnecke, Institute of Geophysics and Planetary Physics, University of California, Los Angeles, Los Angeles, CA 90095-1567. (e-mail: mkivelson@igpp.ucla.edu)

J. A. Linker, Science Applications International Corporation, 10260 Campus Point Drive, MS C-2, San Diego, CA 92121-1578.

C. Polanskey, Jet Propulsion Laboratory, 4800 Oak Grove Avenue, Pasadena, CA 91109

(Received September 22, 1997; revised December 23, 1997; accepted January 13, 1998.)